

Did we hear the sound of the Universe boiling?

Analysis using the full fluid velocity profiles and NANOGrav 15-year data

Tathagata Ghosh,^a Anish Ghoshal,^b Huai-Ke Guo,^c Fazlollah Hajkarim,^d Stephen F King,^e Kuver Sinha,^d Xin Wang,^e Graham White,^e

^aHarish-Chandra Research Institute, A CI of Homi Bhabha National Institute, Chhatnag Road, Jhusi, Prayagraj 211019, India

^bInstitute of Theoretical Physics, Faculty of Physics, University of Warsaw, ul. Pasteura 5, 02-093 Warsaw, Poland

^cInternational Centre for Theoretical Physics Asia-Pacific, University of Chinese Academy of Sciences, 100190 Beijing, China

^dHomer L. Dodge Department of Physics and Astronomy, University of Oklahoma, Norman, OK 73019, USA

^eSchool of Physics and Astronomy, University of Southampton, Southampton SO17 1BJ, United Kingdom

E-mail: tathagataghosh@hri.res.in, anish.ghoshal@fuw.edu.pl, guohuaike@ucas.ac.cn, fazlollah.hajkarim@ou.edu, king@soton.ac.uk, kuver.sinha@ou.edu, Xin.Wang@soton.ac.uk, g.a.white@soton.ac.uk

Abstract. In this paper, we analyse sound waves arising from a cosmic phase transition where the full velocity profile is taken into account as an explanation for the gravitational wave spectrum observed by multiple pulsar timing array groups. Unlike the broken power law used in the literature, in this scenario the power law after the peak depends on the macroscopic properties of the phase transition, allowing for a better fit with pulsar timing array (PTA) data. We compare the best fit with that obtained using the usual broken power law and, unsurprisingly, find a better fit with the gravitational wave (GW) spectrum that utilizes the full velocity profile. Even more importantly, the thermal parameters that produce the best fit are quite different. We then discuss models that can produce the best-fit point and complementary probes using CMB experiments and searches for light particles in DUNE, IceCUBE-Gen2, neutrinoless double β -decay, and forward physics facilities (FPF) at the LHC like FASER ν , etc.

Contents

1	Introduction	1
2	PTA data and the sound shell model	2
3	BSM Scenarios and Complementary Laboratory Probes	4
4	Discussions and Conclusions	8
A	Scanning plots	9

1 Introduction

It has been known for some time that Pulsar Timing Array (PTA) experiments can be used to detect gravitational waves (GWs) [1–3]. This is possible by studying the timing distortions of successive light pulses emitted by millisecond pulsars, which are extremely stable clocks. The PTAs search for spatially correlated fluctuations in the pulse arrival time measurements of such pulsars, due to GWs perturbing the space-time metric along the line of sight to each pulsar. For GWs, the timing distortions should exhibit the angular dependence expected for an isotropic background of spin two GWs which enables them to be distinguished from either spin-zero or spin-one waves, and other effects, according to the work of Hellings and Down [4].

Recently, several PTA projects have reported the discovery of a stochastic gravitational wave background (SGWB). In particular, the North American Nanohertz Observatory for Gravitational Waves (NANOGrav) [5], the European PTA [6], the Parkes PTA [7] and the Chinese CPTA [8] have all released results which seem to be consistent with a Hellings-Downs pattern in the angular correlations which is characteristic of the SGWB. In particular, the largest statistical evidence for SGWB is seen in the NANOGrav 15-year data (NANOGrav15) [5]. This is the first discovery of GWs in the frequency around 10^{-8} Hz, and wavelengths around 10 light years. The most obvious origin of such an SGWB is due to the merging supermassive black hole binaries (SMBHBs) resulting from the collision of two galaxies, each with an SMBH with masses in the range 10^{8-9} solar masses at its centre [9, 10]. The expected amplitude has an order of magnitude uncertainty depending on the density, redshift, and other properties of SMBH sources. Indeed, there may be millions of such sources contributing to the SGWB.

However, the current data does not allow individual SMBH binary sources to be identified, so it is unclear if the observed SGWB has an astrophysical or cosmological origin [11, 12]. For example, the cosmological origin of SGWB could be due to first-order phase transitions [13–19], cosmic strings [20–26], domain walls [27–29], or scalar-induced gravitational waves (SIGWs) generated from primordial fluctuations [30–36]. Such possibilities represent new physics beyond the standard model (BSM) and it would be interesting to know how such alternative scenarios could be distinguished.

One characteristic feature is the shape of the spectrum in the recent data, which, unlike the previous results, seems to be blue-tilted [5, 11]. The analysis of the NANOGrav 12.5-year data release suggested a nearly flat GW spectrum as a function of frequency (f), $\Omega_{GW} \propto f^{(-1.5, 0.5)}$ at one sigma, in a narrow range of frequencies around 5.5 nHz [37]. By contrast,

the recent 15-year data release finds a steeper slope, $\Omega_{GW} \propto f^{(1.3,2.4)}$ at one sigma [5]. The naive scaling predicted for GW from SMBH binaries is disfavoured by the latest NANOGrav data, although environmental and statistical effects can lead to different predictions [11, 38].

Motivated by the above considerations, new analyses are necessary to explore which SGWB formation mechanisms can lead to the generation of a signal consistent with these updated observations. Indeed, following the recent announcements, several papers have appeared which address some of these issues [39–67, 67–71].

In this paper, we consider the sound waves arising from a cosmic phase transition where the full velocity profile is taken into account. We compare the best fit with that obtained using the usual broken power law and find a better fit to NANOGrav data using the full velocity profile. We first explain how to obtain this result before discussing some models that can produce such thermal parameters. Finally, we discuss complementary probes of hidden sectors.

2 PTA data and the sound shell model

Multiple PTA collaborations observed compelling evidence¹ for a gravitational wave spectrum, with NANOGrav and EPTA giving the best fit for a power law spectrum parametrized as follows,

$$\Omega = \frac{8\pi^4 f^5 \Phi(f)}{H_0^2 \Delta f} \quad (2.1)$$

with

$$\Phi = \frac{A^2}{12\pi^2 T_{\text{obs}}} \left(\frac{f}{\text{yr}^{-1}} \right)^{-\gamma} \text{yr}^3 \quad (2.2)$$

where $\Delta f = 1/T_{\text{obs}}$ and $H_0 = h \times 100 \text{ km s}^{-1} \text{ Mpc}^{-1}$ is the current value of the Hubble rate. The best fit values of the parameters A and γ in Eq. 2.2 are given by

$$\gamma = \begin{cases} 3.2 \pm 0.6 & \text{NANOGrav} \\ 3.1_{-0.68}^{+0.77} & \text{EPTA} \end{cases} \quad (2.3)$$

$$A = \begin{cases} 6.4_{-2.7}^{+4.2} \times 10^{-15} & \text{NANOGrav} \\ 10^{-14.13 \pm 0.12} & \text{EPTA} \end{cases} \quad (2.4)$$

While inspiralling SMBHBs provide the standard astrophysical explanation for the signal, a first-order phase transition (FOPT) at the $\mathcal{O}(\text{MeV})$ scale is an intriguing alternative. In this Section, we model the FOPT with the sound shell model [72], obtain the corresponding GW spectrum, and compare our results with the fit performed by the NANOGrav Collaboration.

The GW spectrum from a FOPT is characterized by the following parameters: the nucleation temperature T_n , the strength of the FOPT α_n , the average separation of bubbles R_n which can be related to the bubble nucleation rate β , and the bubble wall velocity v_w . The fit frequently appearing in the literature, and in particular in the recent analysis of the NANOGrav paper describes a single broken power-law of the form [72–79]

$$h^2 \Omega_{\text{GW}} = 2.5 \times 10^{-6} \left(\frac{100}{g_*(T_e)} \right)^{1/3} \Gamma^2 \bar{U}_f^4 \left[\frac{H_s}{\beta(v_w)} \right] v_w \times \Upsilon \times S(f), \quad (2.5)$$

¹The goal of our paper is to assume that the evidence is robust and then ask the following theoretical questions: to what extent can the data be explained by incorporating the effect of SMBH binaries; and can one consider a new physics source, especially sound waves of a first order phase transition? The extensive BSM studies performed by the NANOGrav collaboration assume a similar outlook [11].

Full Sound shell		Broken power law fit	
Parameter	Best fit value	Parameter	Best fit value
α_n	0.85	α_n	0.89
β/H_*	42	β/H_*	5.17
T_n	133 MeV	T_n	142 MeV
v_w	0.09	v_w	0.67
χ_{fit}	1.4	χ_{fit}	1.59

Table 1. Best fit values for the full sound shell model and the usual fit used in the literature as given by Eq. 2.5. The full sound shell model performs somewhat better than the fit.

where \bar{U}_f is the root mean square fluid velocity, $\Gamma \sim 4/3$ is the adiabatic index and Υ is the suppression factor arising from the finite lifetime [73, 80] (τ_{sh}) of the sound waves [73]

$$\Upsilon = 1 - \frac{1}{\sqrt{1 + 2\tau_{\text{sh}}H_s}}. \quad (2.6)$$

Finally, the spectral form has the shape

$$S(f) = \left(\frac{f}{f_p}\right)^3 \left(\frac{7}{4 + 3(f/f_p)^2}\right)^{7/2} \quad (2.7)$$

where f_p is the peak frequency given by

$$f_p = 8.9 \times 10^{-6} \frac{1}{v_w} \left(\frac{\beta}{H_e}\right) \left(\frac{z_p}{10}\right) \left(\frac{T_e}{100\text{GeV}}\right) \left(\frac{g_*(T_e)}{100}\right)^{1/6} \text{ Hz} \quad (2.8)$$

However, a full calculation of the sound shell model can see qualitative deviations from this curve [78] with a better fit being a double broken power law. Most important for our interests is the fact that the power law after the peak depends on the strength of the phase transition and the bubble wall velocity [81]. A more optimistic scenario was studied in [11] where the power law on either side of the peak was treated as a free parameter. In this work, we will perform a full calculation of the sound shell model to take advantage of this flexibility in the peak of the spectrum. Note that in the sound shell model, by keeping the force term between the bubble wall and the plasma longer, the shape can be modified in the infrared [82].

We perform a scan over the space of thermal parameters, $(\alpha_n, T_n, v_w, \beta/H_n)$, to find the best fit to the NANOGrav data (who have released their full data including uncertainties). The scans are performed over the following ranges: nucleation temperature $3 \text{ MeV} < T_n < 150 \text{ MeV}$, bubble wall velocity $0 < v_w < 1$, phase transition strength $0 < \alpha_n < 1$, and the efficiency of bubble formation w.r.t. the expansion rate $0 < \beta/H < 100$. Since the relevant ranges of temperature and frequency are around the quark-gluon confinement regime near 150 MeV, we consider $g_*(T_n)$ the evolution of degrees of freedom for the energy density of the thermal bath of SM particles at the nucleation temperature [83]. The best fit point we use the following figure of merit

$$\chi_{\text{fit}}^2 = \sum_{i=1}^N \frac{(\log_{10} \Omega_{\text{th}} h^2 - \log_{10} \Omega_{\text{exp}} h^2)^2}{2\sigma_i^2}, \quad (2.9)$$

where $\Omega_{\text{th}} h^2$ and $\Omega_{\text{exp}} h^2$ represent the GW relic from theoretical prediction of FOPT and experimental value from PTA, respectively. Note that we ignore the width in the uncertainty

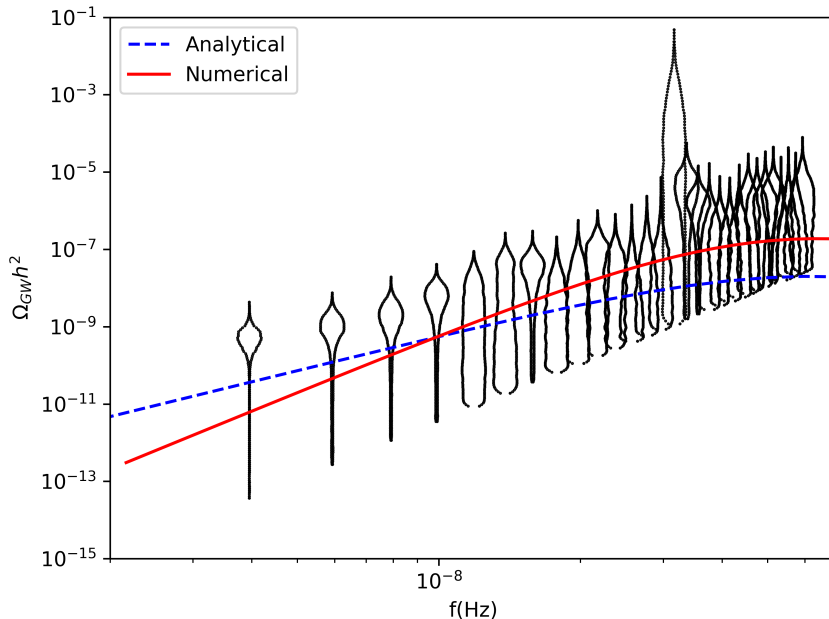


Figure 1. The data from NANOGrav measurement for relic density of SGWB w.r.t. frequency in Hz (black) against the best fit using the full sound shell model (red) and the best fit for a broken power law fit (blue) frequently appearing in the literature (see eqn 2.5). The parameters behind each fit are in Table 1.

regions, taking the midpoint and fitting to the vertical width. That is, σ , in the above equation is the distance from the midpoint value of $\log_{10} h^2 \Omega_{\text{GW}}$ for each uncertainty region to the top or bottom. The best fit value of GW spectrum from our scan along with NANOGrav data are shown in figure 3.

To demonstrate the difference in preferred thermal parameters, in Fig. 2 we fix two thermal parameters to their best fit values and vary β/H_* and T_n . The numerical scan prefers much more realistic values, slightly larger β/H_* (it takes quite a fine tuned supercooling to go lower) and a temperature around the QCD transition. Using the data of NANOGrav we obtain the following values for the best fit point: $v_w \simeq 0.09$, $\alpha_n \simeq 0.85$, $T_n \simeq 132.95$ MeV and $\beta/H \simeq 42.02$. One note of caution, this is in the parameter range where there should be a large suppression due to energy lost to vorticity [84]. In Appendix A, we show that this is somewhat mitigated by the fact that there are good fits which have a smaller trace anomaly and larger velocity.

3 BSM Scenarios and Complementary Laboratory Probes

We are somewhat spoilt for choice in models that can produce a strong first order phase transition at roughly the QCD scale. The very large strength of the transition lends credit to solitosynthesis as a possible explanation [85], as this mechanism typically leads to a stronger transition than conventional nucleation. The low wall velocity, however, supports a model that can predict a lot of friction like perhaps a SIMP model which can contain particles with large multiplicites [86–89]. Quite a few other dark sector phase transitions have been

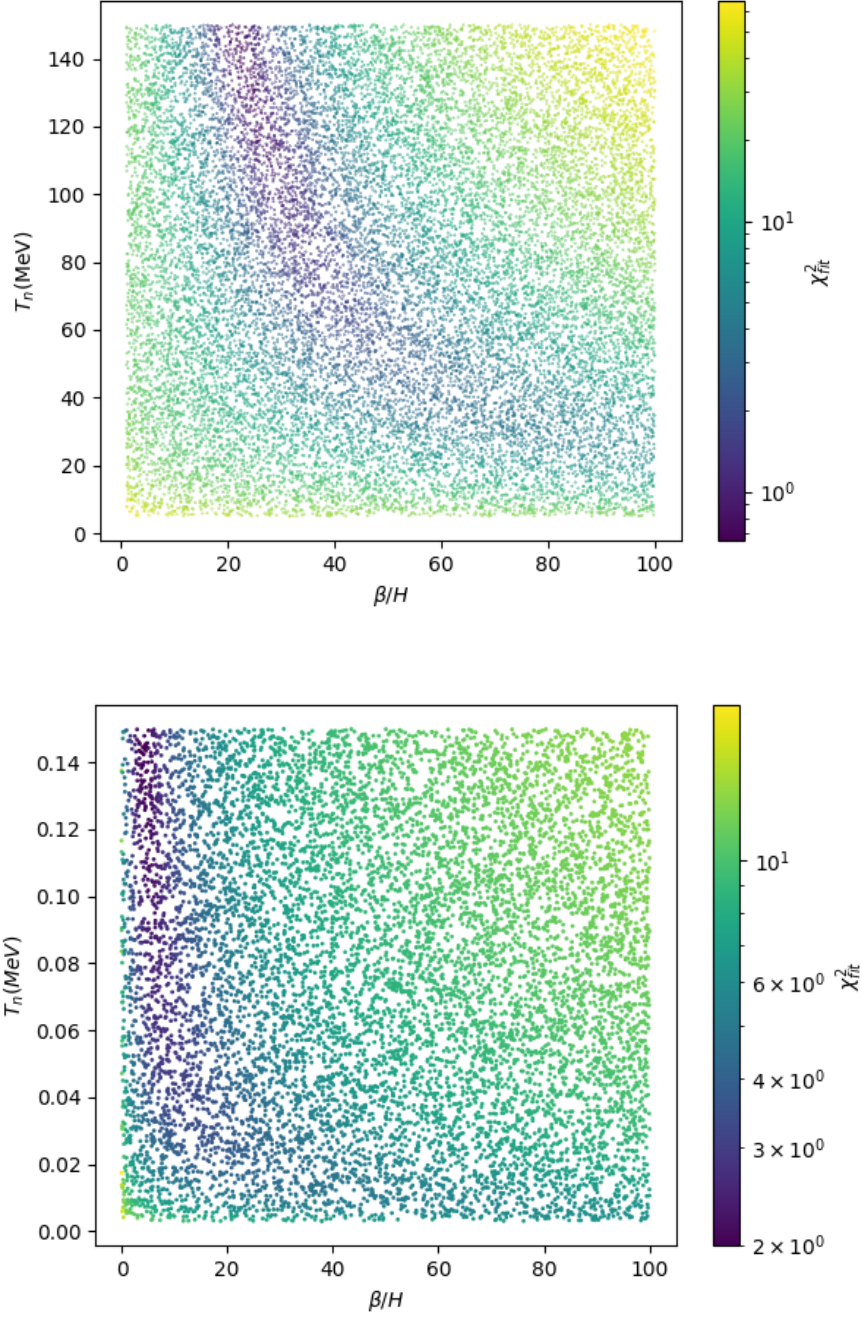


Figure 2. Scan over $(\beta/H_*, T_n)$ with (α, v_w) set to their best fit values for the full velocity profile (top panel) versus the broken power law fit (bottom panel). The fit favours problematic points with very small values for both parameters, with some parts of the preferred parameter space possibly threatening the fidelity of BBN, whereas the numerical calculation favours slightly larger values of β/H_* and T_n near the QCD transition.

considered in this temperature range, see for instance [90–95]. Of course, while the QCD phase transition is a crossover in the standard model at low density, a high lepton asymmetry or a different number of light quarks can change this picture [96–98]. We focus here on a dark sectors that have the prospect of having complementary probes in searches for long lived particles. A full model survey we leave for future work.

Let us now briefly discuss model-independent constraints on a MeV scale FOPT in the dark or hidden sector. During a FOPT, the vacuum energy contained in the false vacuum gets released, and a part of it goes into reheating the photons or neutrinos in the plasma. The released energy may also end up heating relativistic particles in the dark sector. If the reheating of the SM particles happens at around or after the thermal decoupling of neutrinos and photons, either or both of their temperatures will differ from the predictions of standard cosmology. This will change the relativistic degrees of freedom, N_{eff} , which is strongly constrained by Big Bang Nucleosynthesis (BBN) and the Cosmic Microwave Background (CMB). The abundances of light element will also be modified and offer further bounds. N_{eff} measurements severely constrain the dark sector reheating scenario as well. While our best fit point has a percolation temperature well above the scale at which we need to be concerned with BBN constraints, there are some points that agree well with NANOGrav data and have a much lower percolation temperature. There is a distinction between percolation and nucleation temperatures [74]. For a certain model, these temperatures can vary and produce different results. However, the current study uses a simple bag model for a physics scenario beyond the Standard Model, assuming a first-order phase transition where the nucleation temperature (T_n) is approximately equal to the percolation temperature (T_p). This assumption might change in other models, leading to different outcomes.

We first consider the reheating of the dark radiation case. In the approximation $T_n^D \ll T_n^\gamma$, one can show that $\alpha_n < 0.08$ for $T_n^\gamma \sim \mathcal{O}(\text{MeV})$ [93]. Ref. [93] also derived model-independent constraints on phase temperature (T_n) and strength parameter (α_n) from N_{eff} and helium and primary deuterium abundance ratios (Y_P and $D/H|_P$, respectively) measured by CMB and BBN experiments when the FOPT heats the SM particles. For illustration, we discuss here the neutrino reheating scenario since the portal operator that can induce it (and the associated phenomenology) is relatively well-studied [99]. Ref. [95] explores the timing and temperature of the phase transition (PT) and its potential effects on BBN. Also, the nucleation rate, strength, and inverse duration of the PT are illustrated. The impact of the PT on the effective number of neutrino species (N_{eff}) and neutrino decoupling is a critical concern, especially given the PT’s temperature. However, the PT at temperatures well above the neutrino decoupling (over 100 MeV) does not adversely affect the neutrino-to-photon temperature ratio or increase N_{eff} beyond the acceptable cosmological limits. This is quantified by a function $F(t)$ in Ref. [95] that vanishes depending on the values β/H and T_n . The vanishing of $F(t)$ can safely happen for our best fit points shown in Table 1.

Using the BBN data from PDG [100] and the CMB data from the latest Planck results [101], Ref. [93] shows that the neutrino reheating temperature, T_{rh}^ν , has to be greater than ~ 3 MeV for $\alpha_n > 0.1$. A future CMB experiment like CMB-S4 [102] will improve the bounds to $T_{\text{rh}}^\nu \gtrsim 4$ MeV. One can translate the above bounds on T_{rh}^ν to the phase transition temperature T_n by using the formula,

$$T_{\text{rh}}^\nu = \left[1 + \alpha_n + \alpha_n \frac{g_*^\gamma(t_{\text{rh}})}{g_*^\nu(t_{\text{rh}})} \left(\frac{T_n^\gamma}{T_n^\nu} \right)^4 \right]^{1/4} T_n^\nu, \quad (3.1)$$

where for reheating temperatures above MeV, $g_*^\gamma(t_{\text{rh}}) \approx 11/2$ and $g_*^\nu(t_{\text{rh}}) \approx 21/4$. Thus, one

can conclude that the existing CMB and BBN data bounds place an almost flat constraint on $T_n^\nu \gtrsim 2$ MeV for $\alpha_n > 0.1$ as shown by the blue line in Fig. 1. The bound on T_n from the photon reheating case is almost the same but extends to a bit smaller values of α_n [93]. A cosmic phase transition at temperature T_n can reheat photons and neutrinos in different ways. The neutrino reheating will lead to equal reheating temperatures for photons and neutrinos, potentially resulting in a higher effective neutrino temperature due to the different degrees of freedom [93]. To avoid any problem with the physics of BBN we will consider such a BSM scenario with phase transition.

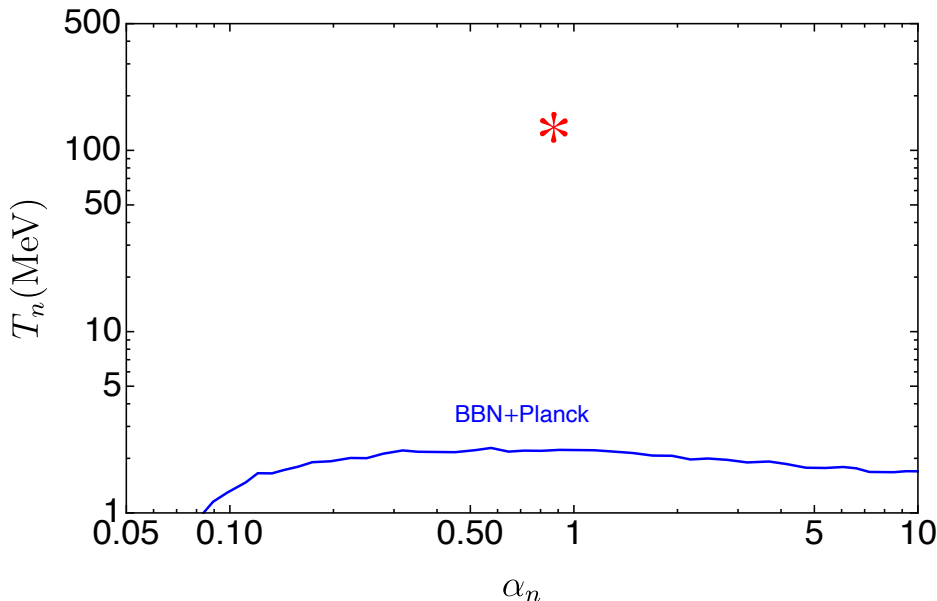


Figure 3. Constraints on FOPT parameters from PLANCK and BBN taken from Ref. [93]. The best-fit point obtained from our sound shell analysis with the NANOGrav data is shown by the red star.

Finally, we provide a brief discussion on the interactions between the SM neutrinos and the dark sector scalar that is responsible for the FOPT under discussion. There is one point that we should clarify that the reheating has to be instantaneous for the above constraints to be applicable. For a delayed reheating, the constraints on the FOPT is expected to be much stronger [93]. The neutrino reheating can happen from the decay of a dark scalar ϕ to a pair of neutrinos via the dimension-6 effective operator

$$\mathcal{O} = \lambda_{\alpha\beta} \frac{(L_\alpha^T i\sigma_2 H)(H^T i\sigma_2 L_\beta)\phi}{\Lambda^2}, \quad (3.2)$$

where L and H are the SM lepton and Higgs doublets, respectively. After the electroweak symmetry breaking the above operator will generate an interaction term $g_{\alpha\beta} \nu\nu\phi$, where $\alpha, \beta = e, \mu, \tau$ and $g_{\alpha\beta} = \lambda_{\alpha\beta} v^2/\Lambda^2$. Significant bounds already exist on the $g_{\alpha\beta} - m_\phi$ plane from existing laboratory experiments like meson decay spectra [103], neutrinoless double β -decay [104], Z or the SM Higgs invisible decay or τ decay [105]. Also, these couplings are of significant interest for study in upcoming experiments like DUNE [106, 107], generation-2 IceCube [108], and forward physics facilities (FPF) [107] at the LHC. We show a subset of these existing and projected bounds on the $g_{\alpha\beta} - m_\phi$ plane in Fig. 4. For the detailed

phenomenology of these couplings at various terrestrial and celestial experiments we refer the interested readers to the recent review paper on this topic [99]. As far as the UV-completion of the effective operator of Eq. 3.2 is concerned, the most canonical models that can provide it are the massive Majoron models [104, 109–111]. In addition, the generation of this effective operator from an inverse seesaw model [112] and a $U(1)_{B-L}$ [113] model has been considered in the literature.

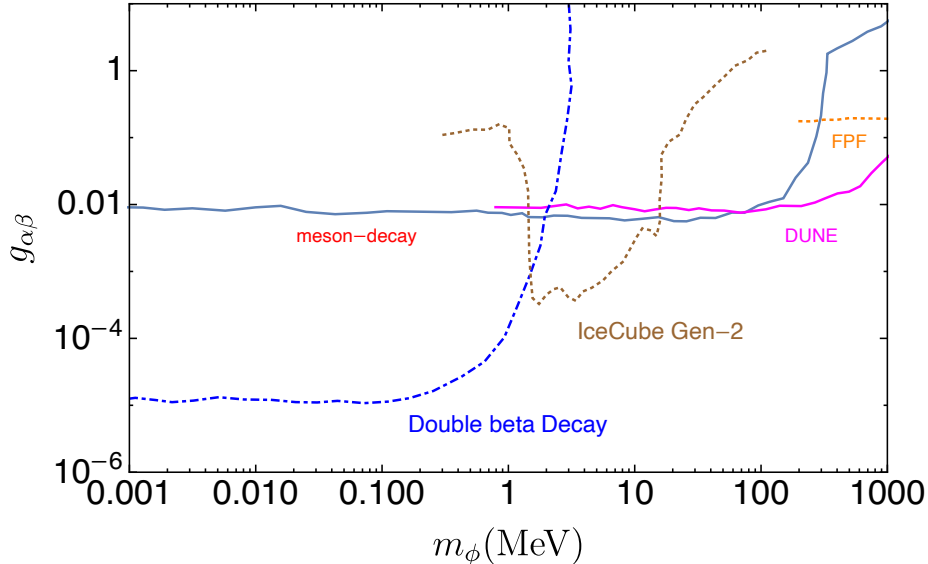


Figure 4. A selection of limits on the parameters $g_{\alpha\beta}$ and m_{ϕ} that can participate in reheating the neutrino plasma from the decay of a dark sector scalar. We show the existing laboratory constraints from meson decay spectra [dark blue solid] and neutrinoless double β -decay [blue dot dashed]. Also we show the projected limits from DUNE [magenta solid], IceCube Gen-2 [brown dotted] and forward physics facility at the LHC [orange dotted].

4 Discussions and Conclusions

In this paper we have had an in depth look at sound wave induced gravitational waves from a strong first order cosmic phase transition as a possible explanation for the recent signal at multiple pulsar timing arrays. In particular, we have looked at how much including the full velocity profile rather than using a broken power law fit improves agreement with data. The best fit parameters also look a bit more realistic than what can be achieved via the broken power law, with the time scale of the phase transition being a smaller fraction of the Hubble time. We of course emphasize the caveat that understanding the spectrum from sound shell models is still in a state of flux. Reheating can suppress the nucleation rate enhancing the spectrum [114]. On the other hand, energy lost to vorticity can suppress the spectrum [84]. We leave a detailed analysis of this to future work. We then took a brief look at dark sector models that can be responsible for such a phase transition. We show that one for phase transitions occurring at low temperatures, the cosmological constraints from BBN, PLANCK data and future sensitivities from CMB experiments like CMB-S4, CMB-HD, CMB-Bharat, LiteBIRD will be complementary to the gravitational wave detectors to essential probe phase transition parameter space. This complementarity approach to probe

phase transitions via GW detectors as well as CMB detectors paves the way distinguish the SMBHB and phase transition explanations to observed gravitational waves. Furthermore we showed that once we fix an operator that decides the interactions between the SM sector and the invisible sector (Eqn. 11) one is able to search for such mediators which is responsible for such interactions. We also discussed possible UV-complete neutrino mass models that can give rise to such low scale phase transitions and GW from sound waves measured in PTA data however detailed analysis involving a complete UV-complete model is beyond the scope of the current paper and will be taken up in a future publication. We envisage that the precision measurements that the GW cosmology and GW astronomy offers us from current data and from the planned worldwide network of GW detectors will make the dream of testing particle physics and fundamental BSM scenarios a reality in the very near future.

Finally, we summarize the possibility of performing precision physics with NANOGrav. At the current level of precision of the data, there are several inputs in the phase transition process that can accommodate large variations. This is already evident from our Table 1, where we display the differences between a precise treatment of the sound shell model versus a fit to the broken power-law. Already at this level of precision, it is evident that there is a substantial difference in the benchmark values of the nucleation temperature, bubble wall velocity, and phase transition duration. In the future era of more data, a precise treatment of the PT will then have to take into account several quantities: (1) source lifetime; (2) mean bubble separation; (3) going beyond the bag model approximation in solving the hydrodynamics equations and explicitly calculating the fraction of energy in the fluid from these equations rather than using a fit; (4) including fits for the energy lost to vorticity modes; (5) including fits for the energy lost to reheating effects; (6) a departure from the "instantaneous reheating" approximation adopted in the study; a careful treatment of the difference between the reheating and nucleation times, and the possibility of the nucleation temperature changing during the reheating process.

Acknowledgments

The work of T.G. is supported by the funding available from the Department of Atomic Energy (DAE), Government of India for Harish-Chandra Research Institute. A.G. thanks hospitality of University of Pisa during the ongoing work. SFK acknowledges the STFC Consolidated Grant ST/L000296/1 and the European Union's Horizon 2020 Research and Innovation programme under Marie Skłodowska-Curie grant agreement HIDDEN European ITN project (H2020-MSCA-ITN-2019//860881-HIDDEN). KS is supported by the U. S. Department of Energy grant DE-SC0009956. XW acknowledges the Royal Society as the funding source of the Newton International Fellowship. We thank Peter Athron for pointing out an error in the prefactor for the analytic fit that has propagated through the literature.

A Scanning plots

In this section we provide more information about the preferred thermal parameter space in the numerical calculation of the soundshell model compared to the analytic fit that arises from taking the RMS fluid velocity. In particular, the wall velocity prefers to be large for the analytic fit to maximize the amplitude of the signal. However, as the shape depends upon the wall velocity and NANOGrav is best fitted to a reasonably gentle slope, the full numerical treatment prefers a relatively small wall velocity, $v_w \lesssim 0.2$.

One note of caution is the best fit values favour a low bubble wall velocity and at least a decent sized trace anomaly. Once the trace anomaly gets large, there is a substantial suppression for small wall velocities due to energy lost to vorticity modes [84]. This is shown in figure 7. This issue is mitigated somewhat by the fact that the χ^2 value remains smaller than the best fit value given by the broken power law even for small values of α . Even still this motivates a detailed simulation to find the true preferred values of thermal parameters. Note that to avoid redundancy, we avoid repeating the plots depicting scans over $(\beta/H_*, T_n)$ which is included in the main body of the paper.

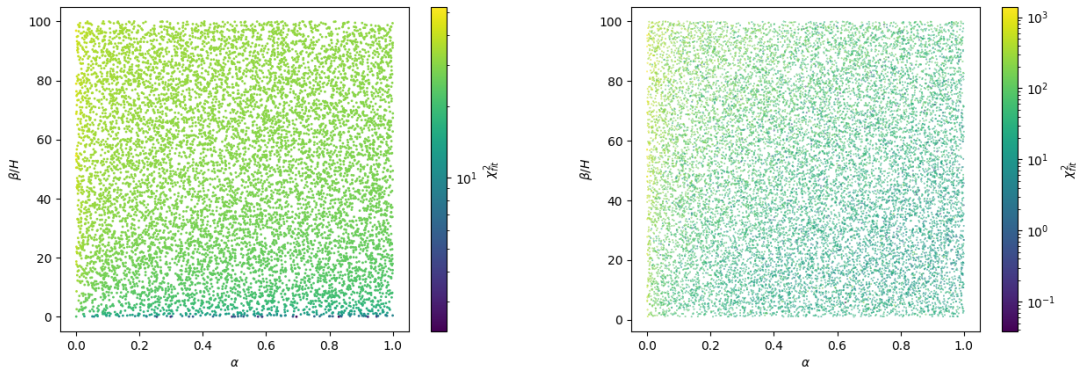


Figure 5. Scan over the thermal parameters $(\alpha, \beta/H_*)$ with (α, v_w) set to their best fit values for the broken power law fit (left panel) and the full numerical treatment of the soundshell model (right panel).

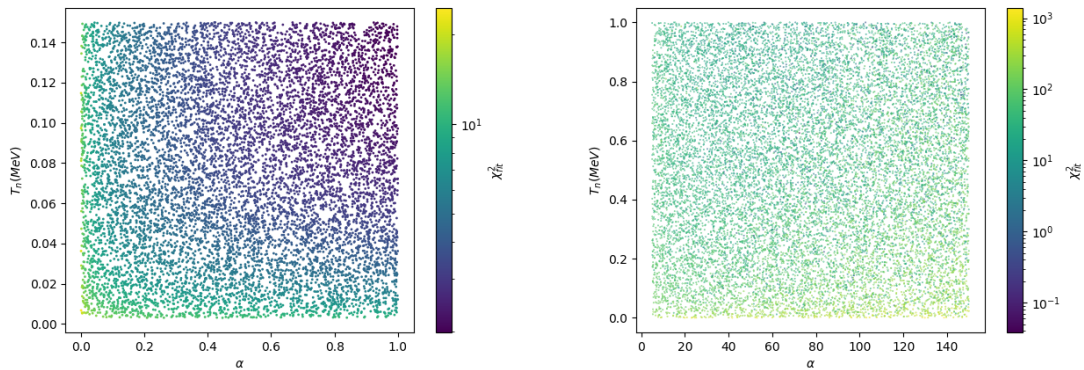


Figure 6. Scan over the thermal parameters (α, T_n) with $(\beta/H_*, v_w)$ set to their best fit values for the broken power law fit (left panel) and the full numerical treatment of the soundshell model (right panel).

References

- [1] M. V. Sazhin, “Opportunities for detecting ultralong gravitational waves,” *Soviet Astronomy* **22** (Feb., 1978) 36–38.

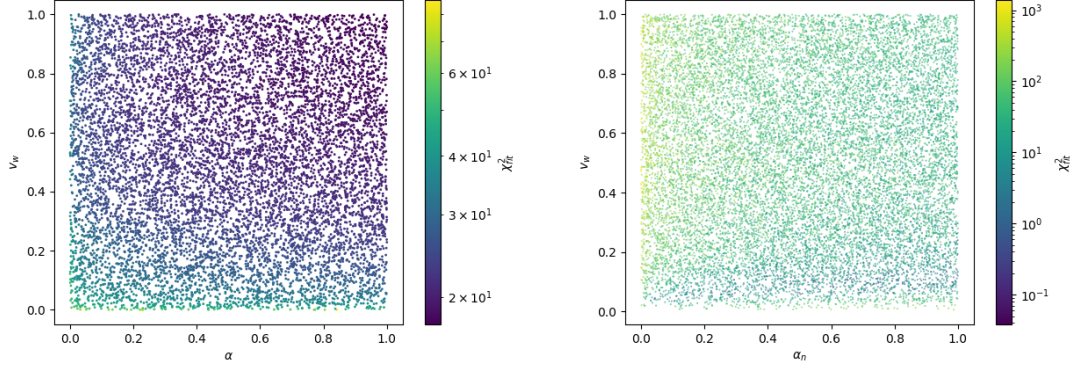


Figure 7. Scan over the thermal parameters (α, v_w) with $(\beta/H_*, T_n)$ set to their best fit values for the broken power law fit (left panel) and the full numerical treatment of the soundshell model (right panel). Note that although the best fit point for the numerical treatment is in the danger region for the suppression factor from energy lost to vorticity modes to be large [84], there are many points with a small χ^2 that have a larger wall velocity and smaller α .

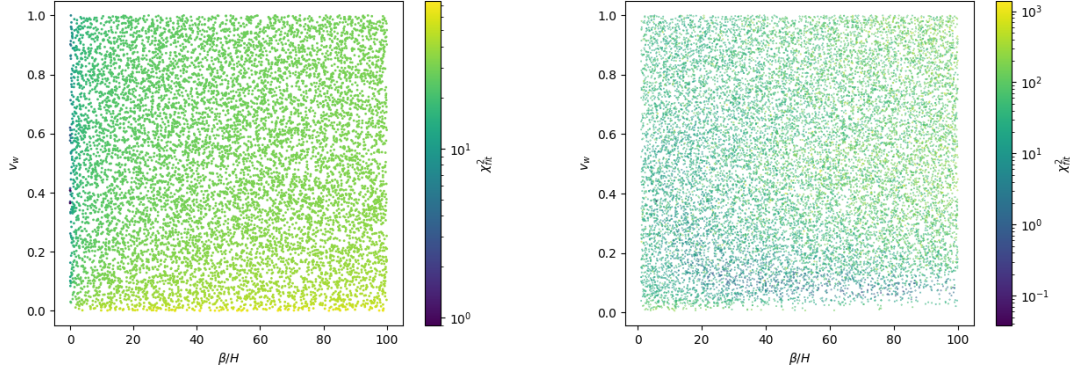


Figure 8. Scan over the thermal parameters $(\beta/H_*, v_w)$ with (α, T_n) set to their best fit values for the broken power law fit (left panel) and the full numerical treatment of the soundshell model (right panel).

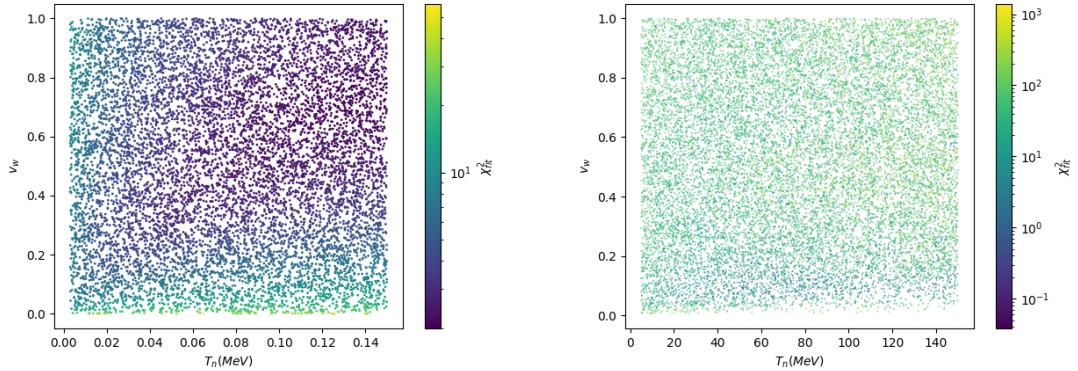


Figure 9. Scan over the thermal parameters (T_n, v_w) with $(\beta/H_*, \alpha)$ set to their best fit values for the broken power law fit (left panel) and the full numerical treatment of the soundshell model (right panel).

- [2] S. L. Detweiler, “Pulsar timing measurements and the search for gravitational waves,” *Astrophys. J.* **234** (1979) 1100–1104.
- [3] R. S. Foster III, *Constructing a pulsar timing array*. University of California, Berkeley, 1990.
- [4] R. w. Hellings and G. s. Downs, “UPPER LIMITS ON THE ISOTROPIC GRAVITATIONAL RADIATION BACKGROUND FROM PULSAR TIMING ANALYSIS,” *Astrophys. J. Lett.* **265** (1983) L39–L42.
- [5] **NANOGrav** Collaboration, G. Agazie *et al.*, “The NANOGrav 15-year Data Set: Evidence for a Gravitational-Wave Background,” *Astrophys. J. Lett.* **951** no. 1, (2023) , [arXiv:2306.16213 \[astro-ph.HE\]](#).
- [6] J. Antoniadis *et al.*, “The second data release from the European Pulsar Timing Array III. Search for gravitational wave signals,” [arXiv:2306.16214 \[astro-ph.HE\]](#).
- [7] D. J. Reardon *et al.*, “Search for an isotropic gravitational-wave background with the Parkes Pulsar Timing Array,” *Astrophys. J. Lett.* **951** no. 1, (2023) , [arXiv:2306.16215 \[astro-ph.HE\]](#).
- [8] H. Xu, S. Chen, *et al.*, “Searching for the nano-hertz stochastic gravitational wave background with the chinese pulsar timing array data release i,” [arXiv:2306.16216 \[astro-ph.HE\]](#).
- [9] A. Sesana, F. Haardt, P. Madau, and M. Volonteri, “Low - frequency gravitational radiation from coalescing massive black hole binaries in hierarchical cosmologies,” *Astrophys. J.* **611** (2004) 623–632, [arXiv:astro-ph/0401543](#).
- [10] S. Burke-Spolaor *et al.*, “The Astrophysics of Nanohertz Gravitational Waves,” *Astron. Astrophys. Rev.* **27** no. 1, (2019) 5, [arXiv:1811.08826 \[astro-ph.HE\]](#).
- [11] **NANOGrav** Collaboration, A. Afzal *et al.*, “The NANOGrav 15 yr Data Set: Search for Signals from New Physics,” *Astrophys. J. Lett.* **951** no. 1, (2023) L11, [arXiv:2306.16219 \[astro-ph.HE\]](#).
- [12] J. Antoniadis *et al.*, “The second data release from the European Pulsar Timing Array: V. Implications for massive black holes, dark matter and the early Universe,” [arXiv:2306.16227 \[astro-ph.CO\]](#).
- [13] J. Winicour, “Gravitational radiation from relativistic phase transitions,” *Astrophysical Journal, Vol. 182, pp. 919-934 (1973)* **182** (1973) 919–934.
- [14] P. Athron, C. Balázs, A. Fowlie, L. Morris, and L. Wu, “Cosmological phase transitions: from perturbative particle physics to gravitational waves,” [arXiv:2305.02357 \[hep-ph\]](#).
- [15] C. Caprini, R. Durrer, and X. Siemens, “Detection of gravitational waves from the QCD phase transition with pulsar timing arrays,” *Phys. Rev. D* **82** (2010) 063511, [arXiv:1007.1218 \[astro-ph.CO\]](#).
- [16] **NANOGrav** Collaboration, Z. Arzoumanian *et al.*, “Searching for Gravitational Waves from Cosmological Phase Transitions with the NANOGrav 12.5-Year Dataset,” *Phys. Rev. Lett.* **127** no. 25, (2021) 251302, [arXiv:2104.13930 \[astro-ph.CO\]](#).
- [17] X. Xue *et al.*, “Constraining Cosmological Phase Transitions with the Parkes Pulsar Timing Array,” *Phys. Rev. Lett.* **127** no. 25, (2021) 251303, [arXiv:2110.03096 \[astro-ph.CO\]](#).
- [18] P. Di Bari, D. Marfatia, and Y.-L. Zhou, “Gravitational waves from first-order phase transitions in Majoron models of neutrino mass,” *JHEP* **10** (2021) 193, [arXiv:2106.00025 \[hep-ph\]](#).
- [19] E. Madge, E. Morgante, C. P. Ibáñez, N. Ramberg, and S. Schenk, “Primordial gravitational waves in the nano-Hertz regime and PTA data – towards solving the GW inverse problem,” [arXiv:2306.14856 \[hep-ph\]](#).

- [20] X. Siemens, V. Mandic, and J. Creighton, “Gravitational wave stochastic background from cosmic (super)strings,” *Phys. Rev. Lett.* **98** (2007) 111101, [arXiv:astro-ph/0610920](#).
- [21] J. Ellis and M. Lewicki, “Cosmic String Interpretation of NANOGrav Pulsar Timing Data,” *Phys. Rev. Lett.* **126** no. 4, (2021) 041304, [arXiv:2009.06555 \[astro-ph.CO\]](#).
- [22] S. F. King, S. Pascoli, J. Turner, and Y.-L. Zhou, “Gravitational Waves and Proton Decay: Complementary Windows into Grand Unified Theories,” *Phys. Rev. Lett.* **126** no. 2, (2021) 021802, [arXiv:2005.13549 \[hep-ph\]](#).
- [23] W. Buchmuller, V. Domcke, and K. Schmitz, “From NANOGrav to LIGO with metastable cosmic strings,” *Phys. Lett. B* **811** (2020) 135914, [arXiv:2009.10649 \[astro-ph.CO\]](#).
- [24] S. Blasi, V. Brdar, and K. Schmitz, “Has NANOGrav found first evidence for cosmic strings?,” *Phys. Rev. Lett.* **126** no. 4, (2021) 041305, [arXiv:2009.06607 \[astro-ph.CO\]](#).
- [25] L. Bian, J. Shu, B. Wang, Q. Yuan, and J. Zong, “Searching for cosmic string induced stochastic gravitational wave background with the Parkes Pulsar Timing Array,” *Phys. Rev. D* **106** no. 10, (2022) L101301, [arXiv:2205.07293 \[hep-ph\]](#).
- [26] B. Fu, A. Ghoshal, and S. King, “Cosmic string gravitational waves from global $U(1)_{B-L}$ symmetry breaking as a probe of the type I seesaw scale,” [arXiv:2306.07334 \[hep-ph\]](#).
- [27] R. Z. Ferreira, A. Notari, O. Pujolas, and F. Rompineve, “Gravitational waves from domain walls in Pulsar Timing Array datasets,” *JCAP* **02** (2023) 001, [arXiv:2204.04228 \[astro-ph.CO\]](#).
- [28] H. An and C. Yang, “Gravitational Waves Produced by Domain Walls During Inflation,” [arXiv:2304.02361 \[hep-ph\]](#).
- [29] D. I. Dunskey, A. Ghoshal, H. Murayama, Y. Sakakihara, and G. White, “GUTs, hybrid topological defects, and gravitational waves,” *Phys. Rev. D* **106** no. 7, (2022) 075030, [arXiv:2111.08750 \[hep-ph\]](#).
- [30] V. Vaskonen and H. Veermäe, “Did NANOGrav see a signal from primordial black hole formation?,” *Phys. Rev. Lett.* **126** no. 5, (2021) 051303, [arXiv:2009.07832 \[astro-ph.CO\]](#).
- [31] V. De Luca, G. Franciolini, and A. Riotto, “NANOGrav Data Hints at Primordial Black Holes as Dark Matter,” *Phys. Rev. Lett.* **126** no. 4, (2021) 041303, [arXiv:2009.08268 \[astro-ph.CO\]](#).
- [32] K. Inomata, M. Kawasaki, K. Mukaida, and T. T. Yanagida, “NANOGrav Results and LIGO-Virgo Primordial Black Holes in Axionlike Curvaton Models,” *Phys. Rev. Lett.* **126** no. 13, (2021) 131301, [arXiv:2011.01270 \[astro-ph.CO\]](#).
- [33] S. Sugiyama, V. Takhistov, E. Vitagliano, A. Kusenko, M. Sasaki, and M. Takada, “Testing Stochastic Gravitational Wave Signals from Primordial Black Holes with Optical Telescopes,” *Phys. Lett. B* **814** (2021) 136097, [arXiv:2010.02189 \[astro-ph.CO\]](#).
- [34] Z. Zhou, J. Jiang, Y.-F. Cai, M. Sasaki, and S. Pi, “Primordial black holes and gravitational waves from resonant amplification during inflation,” *Phys. Rev. D* **102** no. 10, (2020) 103527, [arXiv:2010.03537 \[astro-ph.CO\]](#).
- [35] A. Ghoshal, Y. Gouttenoire, L. Heurtier, and P. Simakachorn, “Primordial Black Hole Archaeology with Gravitational Waves from Cosmic Strings,” [arXiv:2304.04793 \[hep-ph\]](#).
- [36] Z.-C. Chen, C. Yuan, and Q.-G. Huang, “Pulsar Timing Array Constraints on Primordial Black Holes with NANOGrav 11-Year Dataset,” *Phys. Rev. Lett.* **124** no. 25, (2020) 251101, [arXiv:1910.12239 \[astro-ph.CO\]](#).
- [37] **NANOGrav** Collaboration, Z. Arzoumanian *et al.*, “The NANOGrav 12.5 yr Data Set: Search for an Isotropic Stochastic Gravitational-wave Background,” *Astrophys. J. Lett.* **905** no. 2, (2020) L34, [arXiv:2009.04496 \[astro-ph.HE\]](#).

- [38] G. Agazie, A. Anumalapudi, *et al.*, “The nanograv 15-year data set: Constraints on supermassive black hole binaries from the gravitational wave background,” [arXiv:2306.16220 \[astro-ph.HE\]](#).
- [39] S. F. King, D. Marfatia, and M. H. Rahat, “Towards distinguishing Dirac from Majorana neutrino mass with gravitational waves,” [arXiv:2306.05389 \[hep-ph\]](#).
- [40] E. Megias, G. Nardini, and M. Quiros, “Pulsar timing array stochastic background from light kaluza-klein resonances,” [arXiv:2306.17071 \[hep-ph\]](#).
- [41] C. Han, K.-P. Xie, J. M. Yang, and M. Zhang, “Self-interacting dark matter implied by nano-hertz gravitational waves,” [arXiv:2306.16966 \[hep-ph\]](#).
- [42] S.-Y. Guo, M. Khlopov, X. Liu, L. Wu, Y. Wu, and B. Zhu, “Footprints of axion-like particle in pulsar timing array data and jwst observations,” [arXiv:2306.17022 \[hep-ph\]](#).
- [43] J. Yang, N. Xie, and F. P. Huang, “Nano-hertz stochastic gravitational wave background as hints of ultralight axion particles,” [arXiv:2306.17113 \[hep-ph\]](#).
- [44] N. Kitajima, J. Lee, K. Murai, F. Takahashi, and W. Yin, “Nanohertz gravitational waves from axion domain walls coupled to qcd,” [arXiv:2306.17146 \[hep-ph\]](#).
- [45] Y. Bai, T.-K. Chen, and M. Korwar, “Qcd-collapsed domain walls: Qcd phase transition and gravitational wave spectroscopy,” [arXiv:2306.17160 \[hep-ph\]](#).
- [46] L. Zu, C. Zhang, Y.-Y. Li, Y.-C. Gu, Y.-L. S. Tsai, and Y.-Z. Fan, “Mirror qcd phase transition as the origin of the nanohertz stochastic gravitational-wave background detected by the pulsar timing arrays,” [arXiv:2306.16769 \[astro-ph.HE\]](#).
- [47] N. Kitajima and T. Takahashi, “Stochastic gravitational wave background from early dark energy,” [arXiv:2306.16896 \[astro-ph.CO\]](#).
- [48] S. Vagnozzi, “Inflationary interpretation of the stochastic gravitational wave background signal detected by pulsar timing array experiments,” [arXiv:2306.16912 \[astro-ph.CO\]](#).
- [49] G. Lambiase, L. Mastrototaro, and L. Visinelli, “Astrophysical neutrino oscillations after pulsar timing array analyses,” [arXiv:2306.16977 \[astro-ph.HE\]](#).
- [50] J. Ellis, M. Fairbairn, G. Hütsi, J. Raidal, J. Urrutia, V. Vaskonen, and H. Veermäe, “Gravitational waves from SMBH binaries in light of the nanograv 15-year data,” [arXiv:2306.17021 \[astro-ph.CO\]](#).
- [51] Y. Li, C. Zhang, Z. Wang, M. Cui, Y.-L. S. Tsai, Q. Yuan, and Y.-Z. Fan, “Primordial magnetic field as a common solution of nanohertz gravitational waves and hubble tension,” [arXiv:2306.17124 \[astro-ph.HE\]](#).
- [52] G. Franciolini, D. Racco, and F. Rompineve, “Footprints of the qcd crossover on cosmological gravitational waves at pulsar timing arrays,” [arXiv:2306.17136 \[astro-ph.CO\]](#).
- [53] Z.-Q. Shen, G.-W. Yuan, Y.-Y. Wang, and Y.-Z. Wang, “Dark matter spike surrounding supermassive black holes binary and the nanohertz stochastic gravitational wave background,” [arXiv:2306.17143 \[astro-ph.HE\]](#).
- [54] J. Ellis, M. Lewicki, C. Lin, and V. Vaskonen, “Cosmic superstrings revisited in light of nanograv 15-year data,” [arXiv:2306.17147 \[astro-ph.CO\]](#).
- [55] G. Franciolini, A. J. Iovino, V. Vaskonen, and H. Veermäe, “The recent gravitational wave observation by pulsar timing arrays and primordial black holes: the importance of non-gaussianities,” [arXiv:2306.17149 \[astro-ph.CO\]](#).
- [56] Z. Wang, L. Lei, H. Jiao, L. Feng, and Y.-Z. Fan, “The nanohertz stochastic gravitational-wave background from cosmic string loops and the abundant high redshift massive galaxies,” [arXiv:2306.17150 \[astro-ph.HE\]](#).

- [57] A. Ghoshal and A. Strumia, “Probing the dark matter density with gravitational waves from super-massive binary black holes,” [arXiv:2306.17158](#) [[astro-ph.CO](#)].
- [58] K. Fujikura, S. Girmohanta, Y. Nakai, and M. Suzuki, “Nanograv signal from a dark conformal phase transition,” [arXiv:2306.17086](#) [[hep-ph](#)].
- [59] P. Athron, A. Fowlie, C.-T. Lu, L. Morris, L. Wu, Z. Xu, and Y. Wu, “Can Supercooled Phase Transitions explain the Gravitational Wave Background observed by Pulsar Timing Arrays?,” [arXiv:2306.17239](#) [[hep-ph](#)].
- [60] N. Kitajima and K. Nakayama, “Nanohertz gravitational waves from cosmic strings and dark photon dark matter,” [arXiv:2306.17390](#) [[hep-ph](#)].
- [61] G. Lazarides, R. Maji, and Q. Shafi, “Superheavy quasi-stable strings and walls bounded by strings in the light of NANOGrav 15 year data,” [arXiv:2306.17788](#) [[hep-ph](#)].
- [62] A. Yang, J. Ma, S. Jiang, and F. P. Huang, “Implication of nano-Hertz stochastic gravitational wave on dynamical dark matter through a first-order phase transition,” [arXiv:2306.17827](#) [[hep-ph](#)].
- [63] A. Addazi, Y.-F. Cai, A. Marciano, and L. Visinelli, “Have pulsar timing array methods detected a cosmological phase transition?,” [arXiv:2306.17205](#) [[astro-ph.CO](#)].
- [64] T. Broadhurst, C. Chen, T. Liu, and K.-F. Zheng, “Binary Supermassive Black Holes Orbiting Dark Matter Solitons: From the Dual AGN in UGC4211 to NanoHertz Gravitational Waves,” [arXiv:2306.17821](#) [[astro-ph.HE](#)].
- [65] Y.-F. Cai, X.-C. He, X. Ma, S.-F. Yan, and G.-W. Yuan, “Limits on scalar-induced gravitational waves from the stochastic background by pulsar timing array observations,” [arXiv:2306.17822](#) [[gr-qc](#)].
- [66] K. Inomata, K. Kohri, and T. Terada, “The Detected Stochastic Gravitational Waves and Sub-Solar Primordial Black Holes,” [arXiv:2306.17834](#) [[astro-ph.CO](#)].
- [67] P. F. Depta, K. Schmidt-Hoberg, and C. Tasillo, “Do pulsar timing arrays observe merging primordial black holes?,” [arXiv:2306.17836](#) [[astro-ph.CO](#)].
- [68] A. Eichhorn, R. R. Lino dos Santos, and J. a. L. Miqueleto, “From quantum gravity to gravitational waves through cosmic strings,” [arXiv:2306.17718](#) [[gr-qc](#)].
- [69] H.-L. Huang, Y. Cai, J.-Q. Jiang, J. Zhang, and Y.-S. Piao, “Supermassive primordial black holes in multiverse: for nano-Hertz gravitational wave and high-redshift JWST galaxies,” [arXiv:2306.17577](#) [[gr-qc](#)].
- [70] Y. Gouttenoire and E. Vitagliano, “Domain wall interpretation of the PTA signal confronting black hole overproduction,” [arXiv:2306.17841](#) [[gr-qc](#)].
- [71] S. Blasi, A. Mariotti, A. Rase, and A. Sevrin, “Axionic domain walls at Pulsar Timing Arrays: QCD bias and particle friction,” [arXiv:2306.17830](#) [[hep-ph](#)].
- [72] M. Hindmarsh, “Sound shell model for acoustic gravitational wave production at a first-order phase transition in the early Universe,” *Phys. Rev. Lett.* **120** no. 7, (2018) 071301, [arXiv:1608.04735](#) [[astro-ph.CO](#)].
- [73] H.-K. Guo, K. Sinha, D. Vagie, and G. White, “Phase Transitions in an Expanding Universe: Stochastic Gravitational Waves in Standard and Non-Standard Histories,” *JCAP* **01** (2021) 001, [arXiv:2007.08537](#) [[hep-ph](#)].
- [74] H.-K. Guo, K. Sinha, D. Vagie, and G. White, “The benefits of diligence: how precise are predicted gravitational wave spectra in models with phase transitions?,” *JHEP* **06** (2021) 164, [arXiv:2103.06933](#) [[hep-ph](#)].
- [75] R. Caldwell *et al.*, “Detection of early-universe gravitational-wave signatures and fundamental physics,” *Gen. Rel. Grav.* **54** no. 12, (2022) 156, [arXiv:2203.07972](#) [[gr-qc](#)].

- [76] J. R. Espinosa, T. Konstandin, J. M. No, and G. Servant, “Energy Budget of Cosmological First-order Phase Transitions,” *JCAP* **06** (2010) 028, [arXiv:1004.4187 \[hep-ph\]](#).
- [77] F. Giese, T. Konstandin, and J. van de Vis, “Model-independent energy budget of cosmological first-order phase transitions—A sound argument to go beyond the bag model,” *JCAP* **07** no. 07, (2020) 057, [arXiv:2004.06995 \[astro-ph.CO\]](#).
- [78] M. Hindmarsh and M. Hijazi, “Gravitational waves from first order cosmological phase transitions in the Sound Shell Model,” *JCAP* **12** (2019) 062, [arXiv:1909.10040 \[astro-ph.CO\]](#).
- [79] M. Hindmarsh, S. J. Huber, K. Rummukainen, and D. J. Weir, “Shape of the acoustic gravitational wave power spectrum from a first order phase transition,” *Phys. Rev. D* **96** no. 10, (2017) 103520, [arXiv:1704.05871 \[astro-ph.CO\]](#). [Erratum: *Phys.Rev.D* 101, 089902 (2020)].
- [80] J. Ellis, M. Lewicki, and J. M. No, “Gravitational waves from first-order cosmological phase transitions: lifetime of the sound wave source,” *JCAP* **07** (2020) 050, [arXiv:2003.07360 \[hep-ph\]](#).
- [81] C. Gowling and M. Hindmarsh, “Observational prospects for phase transitions at LISA: Fisher matrix analysis,” *JCAP* **10** (2021) 039, [arXiv:2106.05984 \[astro-ph.CO\]](#).
- [82] R.-G. Cai, S.-J. Wang, and Z.-Y. Yuwen, “Hydrodynamic sound shell model,” [arXiv:2305.00074 \[gr-qc\]](#).
- [83] M. Drees, F. Hajkarim, and E. R. Schmitz, “The Effects of QCD Equation of State on the Relic Density of WIMP Dark Matter,” *JCAP* **06** (2015) 025, [arXiv:1503.03513 \[hep-ph\]](#).
- [84] D. Cutting, M. Hindmarsh, and D. J. Weir, “Vorticity, kinetic energy, and suppressed gravitational wave production in strong first order phase transitions,” *Phys. Rev. Lett.* **125** no. 2, (2020) 021302, [arXiv:1906.00480 \[hep-ph\]](#).
- [85] D. Croon, A. Kusenko, A. Mazumdar, and G. White, “Solitosynthesis and Gravitational Waves,” *Phys. Rev. D* **101** no. 8, (2020) 085010, [arXiv:1910.09562 \[hep-ph\]](#).
- [86] Y. Hochberg, E. Kuflik, T. Volansky, and J. G. Wacker, “Mechanism for Thermal Relic Dark Matter of Strongly Interacting Massive Particles,” *Phys. Rev. Lett.* **113** (2014) 171301, [arXiv:1402.5143 \[hep-ph\]](#).
- [87] Y. Hochberg, E. Kuflik, and H. Murayama, “SIMP Spectroscopy,” *JHEP* **05** (2016) 090, [arXiv:1512.07917 \[hep-ph\]](#).
- [88] J. Garcia-Bellido, H. Murayama, and G. White, “Exploring the early Universe with Gaia and Theia,” *JCAP* **12** no. 12, (2021) 023, [arXiv:2104.04778 \[hep-ph\]](#).
- [89] N. Chakrabarty, H. Roy, and T. Srivastava, “Single-step first order phase transition and gravitational waves in a SIMP dark matter scenario,” [arXiv:2212.09659 \[hep-ph\]](#).
- [90] M. Breitbach, J. Kopp, E. Madge, T. Opferkuch, and P. Schwaller, “Dark, Cold, and Noisy: Constraining Secluded Hidden Sectors with Gravitational Waves,” *JCAP* **07** (2019) 007, [arXiv:1811.11175 \[hep-ph\]](#).
- [91] Y. Nakai, M. Suzuki, F. Takahashi, and M. Yamada, “Gravitational Waves and Dark Radiation from Dark Phase Transition: Connecting NANOGrav Pulsar Timing Data and Hubble Tension,” *Phys. Lett. B* **816** (2021) 136238, [arXiv:2009.09754 \[astro-ph.CO\]](#).
- [92] W. Ratzinger and P. Schwaller, “Whispers from the dark side: Confronting light new physics with NANOGrav data,” *SciPost Phys.* **10** no. 2, (2021) 047, [arXiv:2009.11875 \[astro-ph.CO\]](#).
- [93] Y. Bai and M. Korwar, “Cosmological constraints on first-order phase transitions,” *Phys. Rev. D* **105** no. 9, (2022) 095015, [arXiv:2109.14765 \[hep-ph\]](#).

- [94] T. Bringmann, P. F. Depta, T. Konstandin, K. Schmidt-Hoberg, and C. Tasillo, “Does NANOGrav observe a dark sector phase transition?,” [arXiv:2306.09411 \[astro-ph.CO\]](#).
- [95] S. Deng and L. Bian, “Constraining low-scale dark phase transitions with cosmological observations,” [arXiv:2304.06576 \[hep-ph\]](#).
- [96] A. Neronov, A. Roper Pol, C. Caprini, and D. Semikoz, “NANOGrav signal from magnetohydrodynamic turbulence at the QCD phase transition in the early Universe,” *Phys. Rev. D* **103** no. 4, (2021) 041302, [arXiv:2009.14174 \[astro-ph.CO\]](#).
- [97] S.-L. Li, L. Shao, P. Wu, and H. Yu, “NANOGrav signal from first-order confinement-deconfinement phase transition in different QCD-matter scenarios,” *Phys. Rev. D* **104** no. 4, (2021) 043510, [arXiv:2101.08012 \[astro-ph.CO\]](#).
- [98] L. Sagunski, P. Schicho, and D. Schmitt, “Supercool exit: Gravitational waves from QCD-triggered conformal symmetry breaking,” *Phys. Rev. D* **107** no. 12, (2023) 123512, [arXiv:2303.02450 \[hep-ph\]](#).
- [99] J. M. Berryman *et al.*, “Neutrino self-interactions: A white paper,” *Phys. Dark Univ.* **42** (2023) 101267, [arXiv:2203.01955 \[hep-ph\]](#).
- [100] **Particle Data Group** Collaboration, P. A. Zyla *et al.*, “Review of Particle Physics,” *PTEP* **2020** no. 8, (2020) 083C01.
- [101] **Planck** Collaboration, N. Aghanim *et al.*, “Planck 2018 results. V. CMB power spectra and likelihoods,” *Astron. Astrophys.* **641** (2020) A5, [arXiv:1907.12875 \[astro-ph.CO\]](#).
- [102] K. Abazajian *et al.*, “CMB-S4 Science Case, Reference Design, and Project Plan,” [arXiv:1907.04473 \[astro-ph.IM\]](#).
- [103] P. S. Pasquini and O. L. G. Peres, “Bounds on Neutrino-Scalar Yukawa Coupling,” *Phys. Rev. D* **93** no. 5, (2016) 053007, [arXiv:1511.01811 \[hep-ph\]](#). [Erratum: *Phys.Rev.D* 93, 079902 (2016)].
- [104] T. Brune and H. Päs, “Massive Majorons and constraints on the Majoron-neutrino coupling,” *Phys. Rev. D* **99** no. 9, (2019) 096005, [arXiv:1808.08158 \[hep-ph\]](#).
- [105] A. de Gouvêa, P. S. B. Dev, B. Dutta, T. Ghosh, T. Han, and Y. Zhang, “Leptonic Scalars at the LHC,” *JHEP* **07** (2020) 142, [arXiv:1910.01132 \[hep-ph\]](#).
- [106] J. M. Berryman, A. De Gouvêa, K. J. Kelly, and Y. Zhang, “Lepton-Number-Charged Scalars and Neutrino Beamstrahlung,” *Phys. Rev. D* **97** no. 7, (2018) 075030, [arXiv:1802.00009 \[hep-ph\]](#).
- [107] K. J. Kelly, F. Kling, D. Tuckler, and Y. Zhang, “Probing neutrino-portal dark matter at the Forward Physics Facility,” *Phys. Rev. D* **105** no. 7, (2022) 075026, [arXiv:2111.05868 \[hep-ph\]](#).
- [108] J. F. Cherry, A. Friedland, and I. M. Shoemaker, “Neutrino Portal Dark Matter: From Dwarf Galaxies to IceCube,” [arXiv:1411.1071 \[hep-ph\]](#).
- [109] I. Z. Rothstein, K. S. Babu, and D. Seckel, “Planck scale symmetry breaking and majoron physics,” *Nucl. Phys. B* **403** (1993) 725–748, [arXiv:hep-ph/9301213](#).
- [110] P.-H. Gu, E. Ma, and U. Sarkar, “Pseudo-Majoron as Dark Matter,” *Phys. Lett. B* **690** (2010) 145–148, [arXiv:1004.1919 \[hep-ph\]](#).
- [111] F. S. Queiroz and K. Sinha, “The Poker Face of the Majoron Dark Matter Model: LUX to keV Line,” *Phys. Lett. B* **735** (2014) 69–74, [arXiv:1404.1400 \[hep-ph\]](#).
- [112] K.-F. Lyu, E. Stamou, and L.-T. Wang, “Self-interacting neutrinos: Solution to Hubble tension versus experimental constraints,” *Phys. Rev. D* **103** no. 1, (2021) 015004, [arXiv:2004.10868 \[hep-ph\]](#).

- [113] P. S. B. Dev, B. Dutta, T. Ghosh, T. Han, H. Qin, and Y. Zhang, “Leptonic scalars and collider signatures in a UV-complete model,” *JHEP* **03** (2022) 068, [arXiv:2109.04490 \[hep-ph\]](#).
- [114] R. Jinno, T. Konstandin, H. Rubira, and J. van de Vis, “Effect of density fluctuations on gravitational wave production in first-order phase transitions,” *JCAP* **12** no. 12, (2021) 019, [arXiv:2108.11947 \[astro-ph.CO\]](#).